Active Touchdown Bearing Control for Recovery of Contact-Free Rotor Levitation in AMB Systems

Peichao Li[a], Necip Sahinkaya[a,b], Patrick Keogh[a]

[a] Department of Mechanical Engineering, University of Bath, Bath BA2 7AY, UK, p.s.keogh@bath.ac.uk
[b] Department of Mechanical and Automotive Engineering, Kingston University, London KT1 2EE, UK

***Abstract*—Control strategies for rotor displacements and transmitted forces in active magnetic bearing (AMB) systems are generally well-developed when the rotor is in contact-free levitation. In such a condition, the rotor/AMB system, the plant to be controlled, is well-defined to use for controller design. However, transient overload conditions or large scale disturbances may cause the rotor to make contact with one or more touchdown bearings (TDBs). The ensuing dynamic response is an effective change to the contact-free plant, which may cause an AMB controller to apply inappropriate forces, causing persistent contact, or even inducing system instability. It is therefore beneficial to restore contact-free levitation as quickly as possible in order that normal operation may resume. This would minimise outage time and also minimise high levels of potentially damaging contact that may be experienced by the TDBs. In this paper, the use of an active TDB is considered for the restoration of contact-free levitation. The contact problem is demonstrated in simulation and also through appropriate control applied in an experimental system. In this system, TDB motion is activated by piezoelectric stack actuators.**

I. INTRODUCTION

The study of the dynamics of a spinning rotor making contact with a stator component has been the subject of numerous publications. There are many ways in which the rotor may interact, including forward whirl rubbing, backward whirl rubbing, combined bouncing and rubbing, and chaotically induced contact. Direct contact will also involve heat generation, which may cause dynamic rotor thermal bending. These effects are possible in any type of rotating machinery.

Specific to rotor/AMB systems, the problem of rotor contact is a critical factor affecting machine operation. In order to cope with the existence of a clearance gap in AMBs, a TDB may prevent excessive rotor excursions. However, the step-like changes in contact force may be large and may also result in significant excitation of rotor dynamics.

A TDB must be able to cope with two basic cases: (a) Rotor drop in which the AMBs no longer function; and (b) Transient overload cases when the AMBs are still functional. In Case (a), a number of authors have addressed the problem, including the assessment of rotor dynamics through experimental tests [1-8]. Although Case (b) has received less attention, it is important to recognise that high TDB contact forces may occur at potentially damaging levels. Also, when contact forces are experienced for any significant period of time, the rotor lateral motion is resisted by an effective high

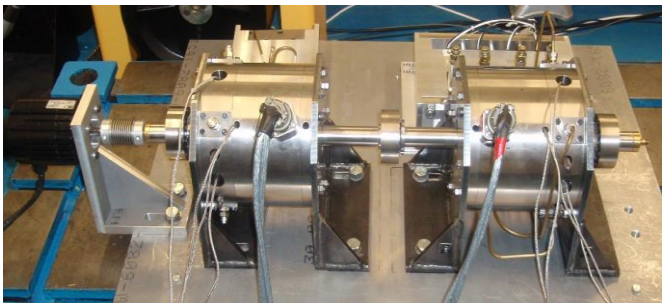

Figure 1. Experimental rotor/AMB/TDB system. The TDBs are adjacent to the AMBs on the outboard sides. The right hand side TDB is actived by piezoelectric actuators.

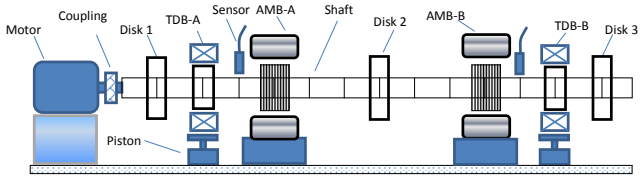

Figure 2. Rotor finite element discretisation for dynamic simulations.

stiffness compared to contact-free operation. Hence, the still functioning AMB controller may react inappropriately to measured rotor displacements. It is easy to envisage that notch filters designed over certain contact-free rotor flexural frequencies may be incorrectly positioned when persistent contact is experienced. This arises due to the changes of rotor dynamic modal frequencies.

A number of authors have recognised the benefits of minimising rotor contact by actively controlling the position of a TDB. In [9, 10], electodynamic actuators are used, though the AMB is not functional. In [11], piezoelectric actuators are used to activate a TDB. That paper focused on the system design to achieve active control of a TDB in orthogonal axes. There is a need to avoid side loads on piezoelectric stack actuators and the use of hydraulic couplings for this purpose is explained in [11], though active control was not applied.

In this paper, the control issues associated with a TDB while the AMBs remain operational are considered. The operating condition of the rotor is taken to be bi-stable with either contact-free levitation or persistent rotor/TDB contact possible. This paper addresses the problem of how to move from the contact to contact-free operation. The bi-stable rotor dynamics are shown experimentally, followed by control back to levitation.

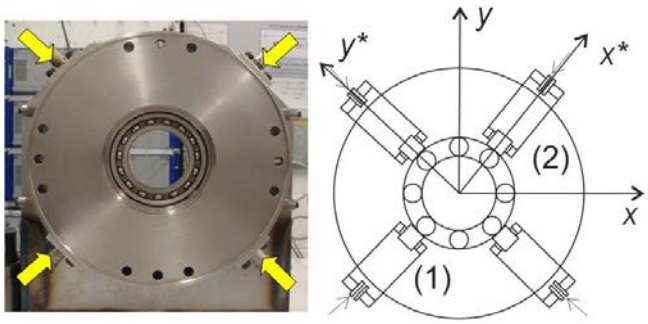

Figure 3. Active TDB system. The TDB is actived by piezoelectric actuators through closed hydraulic lines.

II. EXPERIMENTAL SYSTEM

The rotor/AMB/TDB system used in this study is shown in Fig. 1. For the purposes of dynamic modelling, the rotor is discretised into standard beam elements as shown in Fig. 2. Figure 2 also shows the positions of sensors, AMBs, TDBs, disks and the drive motor. The rotor shaft is 800 mm long. Each AMB has a clearance gap of 0.8 mm. The rolling element TDB shown in Fig. 3 has a radial clearance of 0.4 mm. However, for investigative purposes, TDB bushings were also fabricated with a reduced radial clearance of 0.29 mm. Each AMB has a force capacity of 690 N and break frequency of 250 Hz. The right hand side, non-driven end TDB (TDB-B in Fig. 2) is activated by four 10 kN piezoelectric stack actuators as shown in Fig. 3. The actuators are contained within a manifold (Fig. 4). They are coupled to the TDB through closed hydraulic lines, which prevent damaging side loads from being applied to the actuators.

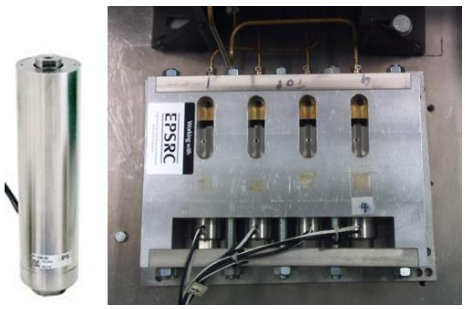

Figure 4. TDB piezoelectric actuator and manifold.

III. SIMULATIONS

A rotor dynamic model of the system was established using the finite element discretisation of Fig. 2. For this section, both TDBs were considered to be in a passive configuration, effectively with the piezoelectric actuators in an 'off' state. The matrix-vector rotor dynamic equation of motion has the form

$$\mathbf{M}\ddot{\mathbf{q}}_r + \mathbf{C}\dot{\mathbf{q}}_r + \mathbf{K}\mathbf{q}_r = \mathbf{f}_m + \mathbf{f}_t + \mathbf{f}_d + \mathbf{f}_u \qquad (1)$$

where $\mathbf{q}_r$ is the rotor displacement vector, $\mathbf{M}$, $\mathbf{C}$ and $\mathbf{K}$ are the mass, damping/gyroscopic and stiffness matrices, $\mathbf{f}_m$, $\mathbf{f}_t$ and $\mathbf{f}_d$ are the AMB, TDB and disturbance force vectors, respectively. $\mathbf{f}_u$ is the unbalance force vector.

The TDB force vector consists of normal and tangential (friction) components as derived from Hertzian contact theory. A coefficient of friction equal to 0.15 was used to evaluate the friction force. For the simulations, the nominal

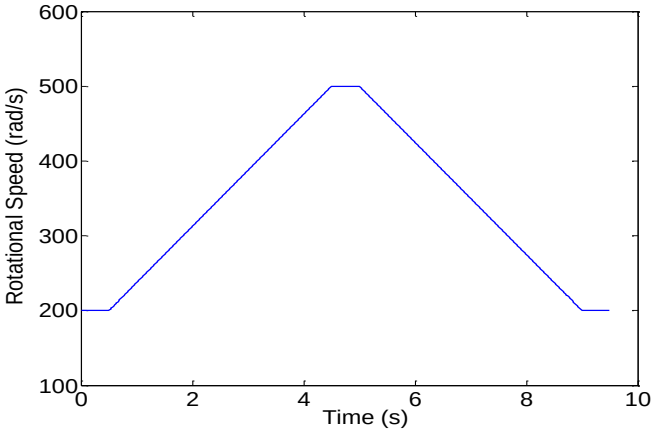

Figure 5. Simulated speed variation with time.

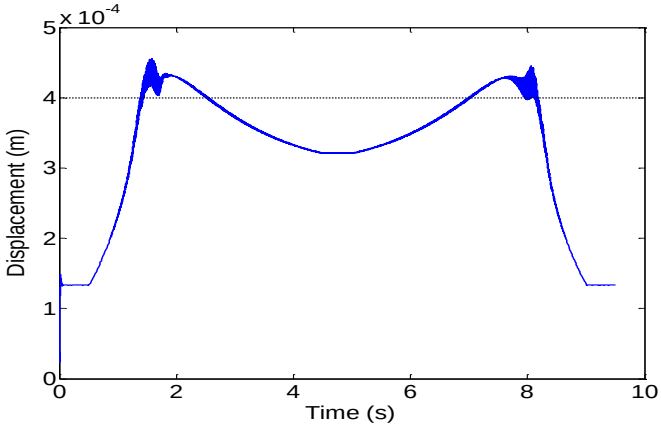

Figure 6. Radial displacement of the rotor at touchdown bearing position assuming that no TDBs are present.

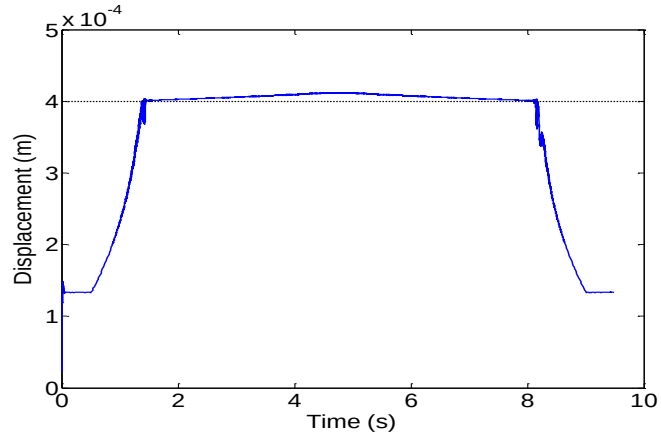

Figure 7. Radial displacement of the rotor at touchdown bearing position. The rotor remains in contact with the TDB for speeds above 270 rad/s.

TDB radial clearance of 0.4 mm was used. Since the TDBs are also moveable, another equation of motion is also formed:

$$\mathbf{M}_t\ddot{\mathbf{q}}_t + \mathbf{C}_t\dot{\mathbf{q}}_t + \mathbf{K}_t\mathbf{q}_t = -\mathbf{f}_t \quad (2)$$

where $\mathbf{q}_t$ is the TDB displacement vector. $\mathbf{M}_t$, $\mathbf{C}_t$ and $\mathbf{K}_t$ are the TDB mass, damping and stiffness matrices that are tailored to match the displacement vectors.

In a simulation with an appropriate unbalance on the end disks (1 and 3 in Fig. 2), the rotor speed was varied according to that shown in Fig. 5. Without consideration of TDBs ($\mathbf{f}_t = \mathbf{0}$), Fig. 6 shows the rotor radial displacement to increase-decrease-increase-decrease as appropriate to passing through a rigid body critical frequency. It is noted that the radial displacement exceeds 0.4 mm in this transition. When the TDBs are included ($\mathbf{f}_t \neq \mathbf{0}$) in the simulation, Fig. 7 shows that rotor contact persists at speeds above 270 rad/s. It may be inferred from Figs 6 and 7 that bi-stable contact and contact-free rotor motions are possible at speeds between 320 rad/s and 500 rad/s.

IV. INDUCED ROTOR/TDB CONTACT TESTS

Since rotor/TDB contact may induce severe vibration, it was decided in the first instance to undertake low speed tests in which variable frequency rotating forces were applied to the rotor through the AMBs. In terms of rotor dynamic response, the gyroscopic moments are negligible, but this may be acceptable if disk conical motions are small. Hence equal in-phase rotating forces were applied through each AMB. Although the rotor is symmetric, the motor coupling caused the orbits at the motor end to be slightly smaller than those at the non-driven end over the range of frequencies applied (up to 450 rad/s). Furthermore, rotor/TDB contact tended to occur at TDB-B.

Initial tests with the rolling element bearing shown in Fig. 3 were problematic with large amplitude rotor vibration experienced. This was attributed to steel-steel friction and excessive inertia in the TDB. It was therefore decided upon to replace the rolling element bearings with bronze bushings. Furthermore, the radial clearance of TDB-B was reduced to 0.29 mm to guarantee that it was the only one to experience contact.

Figure 8 shows the measured maximum rotor radial displacement in the plane of the sensor pair associated with control of AMB-B. This pair is also relatively close to TDB-B (Fig. 2). The rotating forces applied through the AMBs simulate unbalance through speed-frequency association. The frequency was slowly increased from 200 rad/s to 450 rad/s, and then reduced at a similar rate. The regions in which the radial displacements overlap correspond with a non-contacting linear response either side of a resonance (~ 320 rad/s). With frequency increase, contact persists from 310 rad/s to 405 rad/s, before it is lost. As the frequency reduces, the rotor is contact-free up to 360 rad/s, then contact persists down to 300 rad/s after which the rotor becomes contact-free. The hysteresis effect clearly shows that bi-stable rotor dynamics are evident from 300 rad/s to 405 rad/s.

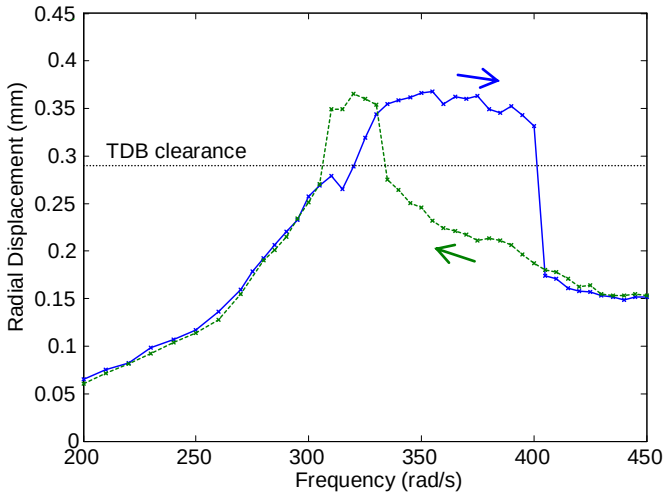

Figure 8. Rotor maximum radial displacement at AMB-B with respect to gradual run up and run down of the rotating force frequency. The rotating forces were equivalent to 500 g.mm and applied in-phase to the rotor through each magnetic bearing.

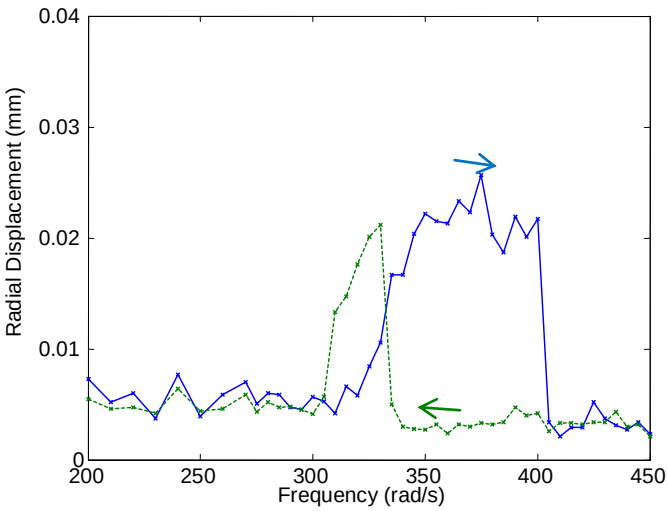

Figure 9. TDB-B maximum radial displacement with respect to gradual run up and run down of the rotating force frequency. The rotating forces were equivalent to 500 g.mm and applied in-phase to the rotor through each magnetic bearing.

A sensor pair was also available to measure the displacement of TDB-B during the frequency tests. Figure 9 also shows the effect of the bi-stable rotor response between 300 rad/s and 405 rad/s. The lower values of maximum radial TDB displacement (around 0.005 mm) correspond with contact-free motion, and are attributable to measurement noise and the eddy current displacement sensor sensitivity.

Figures 10 and 11 show the orbits at the sensor planes associated with the AMB control axes at 335 rad/s and 400 rad/s, respectively. It is noted that the orbits at AMB-B are directionally biased, which is likely due to slight radial misalignment of TDB-B relative to the centre of AMB-B.

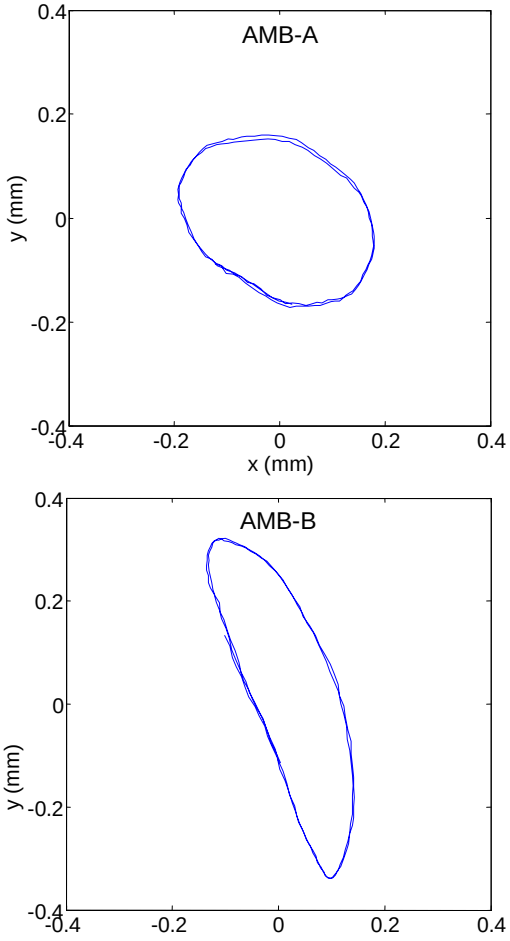

Figure 10. AMB Orbits at 335 rad/s

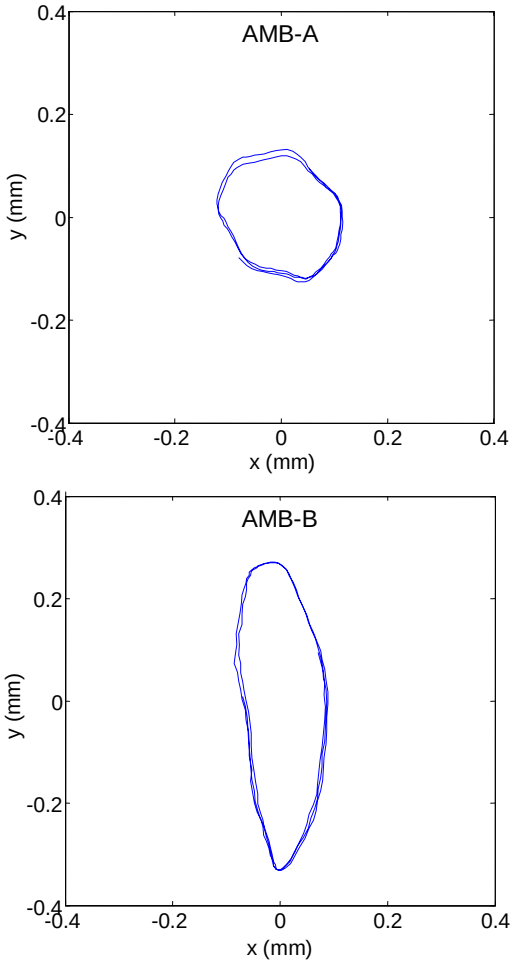

Figure 11. AMB Orbits at 400 rad/s

V. ROTATIONAL TESTS

Frequency based tests have a benefit of being independent of any inherent unbalance in the test rotor. Nonetheless, it is important to assess whether the low speed/frequency variation procedure is acceptable. The rotor was therefore balanced and Disks 1 and 3 were then unbalanced through the addition of in-phase masses (11 g each), equivalent to 500 g.mm. The rotor was then run up slowly in speed to 450 rad/s and then run down.

Figure 12 shows the measured rotor maximum radial displacement at AMB-B. The results correlate well with those of Fig. 8 with similar ranges of bi-stable frequencies and speeds. There is some sensitivity associated with residual unbalance arising from the balancing procedure. However, the results were deemed to be acceptable and indicate that low speed frequency based testing of contact may be a safer alternative to rotational tests, particularly during initial trials.

The corresponding TDB-B maximum radial displacements are shown in Fig. 13. The correlation with Fig. 9 is acceptable in terms of the bi-stable speed and frequency ranges. However, there are differences in profiles. The most notable is the TDB-B maximum radial displacement during

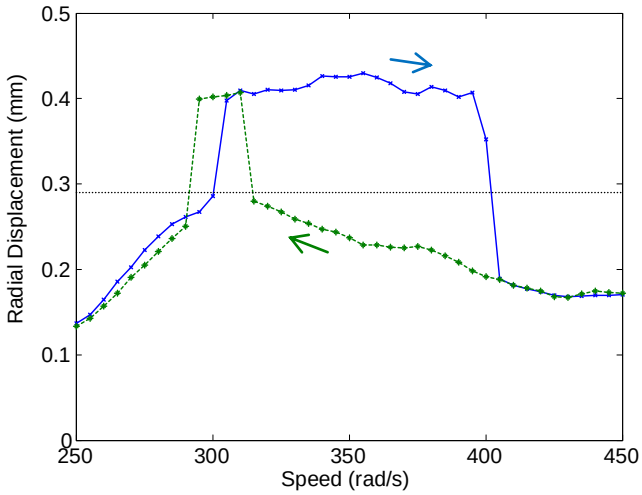

Figure 12. Rotor maximum radial displacement at AMB-B with respect to gradual run up and run down of the rotating speed. The in-phase unbalances of Disks 1 and 3 were 500 g.mm.

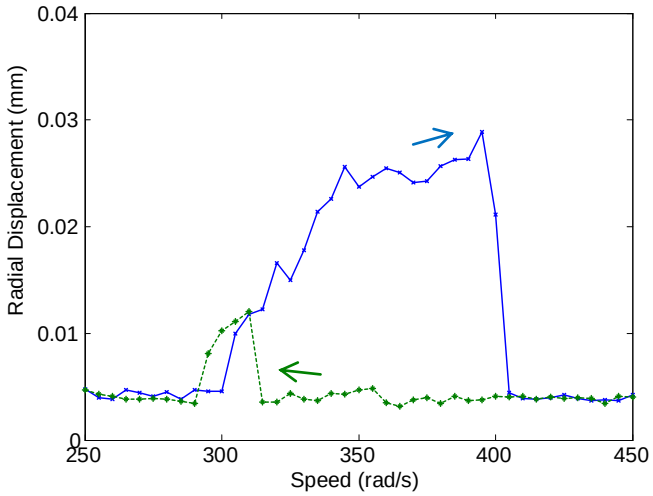

Figure 13. TDB-B maximum radial displacement with respect to gradual run up and run down of the rotating speed. The in-phase unbalances of Disks 1 and 3 were 500 g.mm.

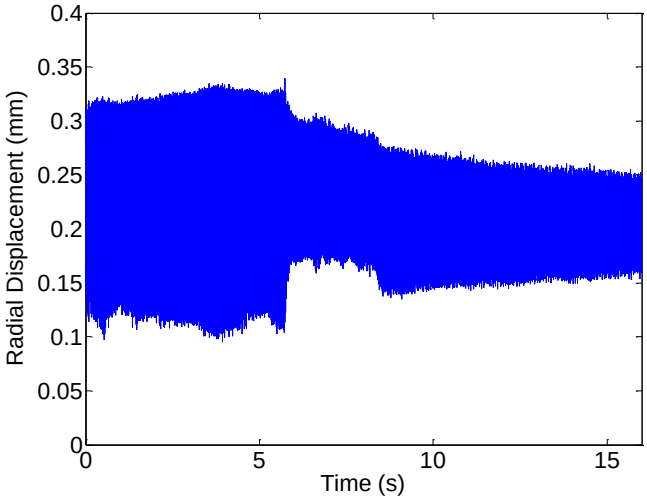

Figure 15. Rotor radial displacement at AMB-B. TDB-B control at frequency 380 rad/s is applied at 6 s to bring rotor out of contact.

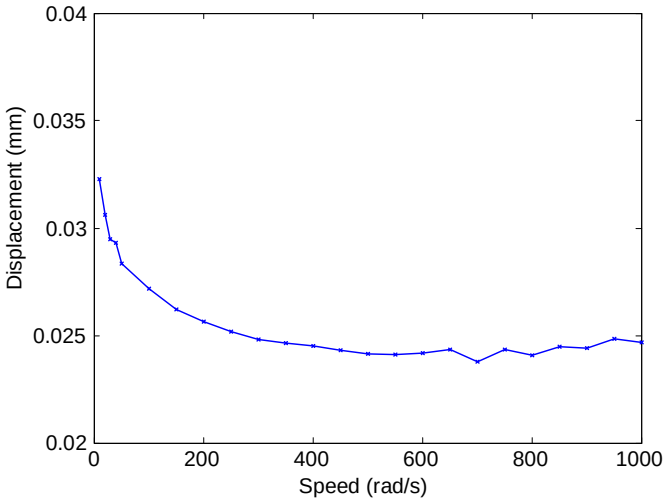

Figure 14. TDB-B average radial displacement when circular orbit demand of radius 0.05 mm is applied.

speed run down attaining 0.012 mm compared with a frequency run down value of 0.021 mm.

VI. RE-LEVITATION AFTER CONTACT

The derivation of a suitable TDB control strategy to move the rotor from a persistent contact condition to a bi-stable contact-free condition is a difficult problem since the plant dynamics depend on frequency/speed. Moreover, the plant dynamics change between the bi-stable states of the rotor. It is also a requirement that the TDB actuation system must be capable of reacting against the induced contact forces and it must not have excessive radial displacement so as to compromise the AMB air gap.

When tested in isolation from the rotor, Fig. 14 shows the effective frequency response of TDB-B under a 0.05 mm radius circular orbit demand. The decay in the response may be due to fluid compressibility in the hydraulic lines together with resistance from the pressurised seals. Notwithstanding this attenuation, this response would be capable of matching the passive displacements experienced by TDB-B in Figs 9 and 13. TDB-B would also maintain an AMB-B airgap.

The control strategy employed was assessed with respect to the rotor dynamic mode at 320 rad/s. The bi-stable modes are dominantly of a rigid body cylindrical nature. It was decided upon to attempt contact-free re-levitation at a frequency of 380 rad/s. An assessment of the nonlinear response indicated that it would be beneficial to move TDB-B in the same sense as the rotor motion in order to reduce contact forces. At other frequencies this may not be beneficial and some phase difference between the rotor and TDB induced motion may be more appropriate. Figure 15 shows the transient response from persistent contact to a contact-free state. The corresponding steady state orbits at AMB-B are shown in Fig. 16,

VII. CONCLUSIONS

It has been demonstrated that bi-stable rotor/TDB contact and contact-free orbits may co-exist under particular operating conditions within a rotor/AMB system. It is shown that for conditions in which gyroscopic moments are small, unbalance response tests may be replaced by low speed tests that utilise rotating forces from AMBs. Similar ranges of bi-stable modes were identified through speed (for unbalance) or frequency (for AMB rotating forces). The low speed tests have a greater margin of safety. They allow the user to prevent potentially destructive contact forces by simply switching off the rotating forces, rather than having to endure speed run-down.

It is always desirable to operate a rotor/AMB/TDB system in a contact-free condition. However, certain bi-stable contact modes may be persistent. This paper shows that relatively small TDB motions, synchronously applied with the rotational frequency/speed and appropriately phased relative to the rotor motion, may be effective in restoring contact-free rotor operation.

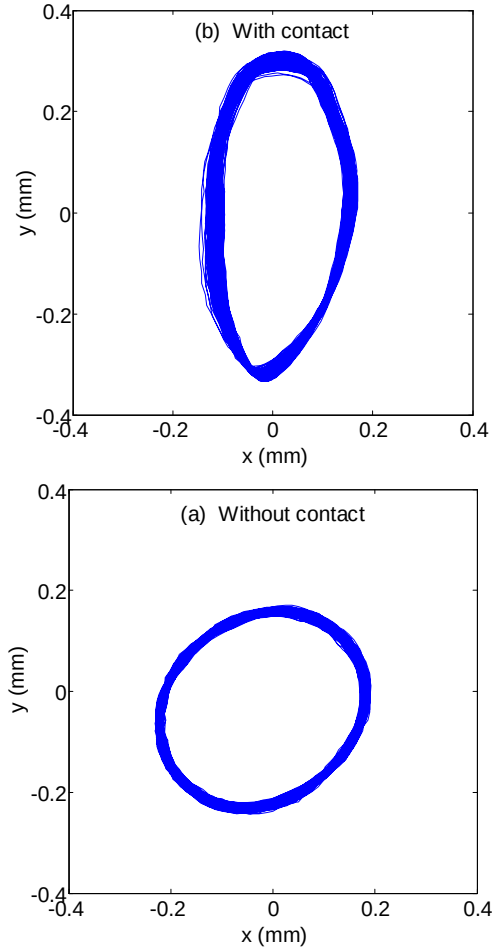

Figure 16. Rotor orbit at AMB-B before (a) and after (b) TDB control was applied at 380 rad/s.

VIII. ACKNOWLEDGEMENT

The authors are grateful for the support of the EPSRC under grant EP/D031389 for the development of the experimental facility. Peichao Li was also supported by a University of Bath research studentship for his PhD study.

REFERENCES

[1] J. Schmied, and J.C. Pradetto, "Behavior of a one ton rotor being dropped into auxiliary bearings," *Proceedings 3rd Int. Symp. Magnetic Bearings*, Alexandria, VA, pp. 145-156, 1992.

[2] R.G. Kirk, and T. Ishii, "Transient response drop analysis of rotors following magnetic bearing power outage," *Proceeding MAG'93*, Alexandria, VA, pp. 53-61, 1993.

[3] R.G. Kirk, E.E. Swanson, F.H. Kavarana, and X. Wang, "Rotor drop test stand for AMB rotating machinery, Part 1: Description of test stand and initial results," *Proceedings 4th Int. Symp. Magnetic Bearings*, ETH Zurich, pp. 207-212, 1994.

[4] E.E. Swanson, R.G. Kirk, and J. Wang, "AMB rotor drop initial transient on ball and solid bearings," *Proceedings MAG'95*, Alexandria, VA, pp. 207-216, 1995.

[5] M. Fumagalli, P. Varadi, and G. Schweitzer, "Impact dynamics of high speed rotors in retainer bearings and measurement concepts," *Proceedings 4th Int. Symp. Magnetic Bearings*, ETH Zurich, pp. 239-244, 1994.

[6] M. Fumagalli, and G. Schweitzer, "Measurements on a rotor contacting its housing," Paper C500/085/96, *Proceedings 6th Int. Conf. Vibrations in Rotating Machinery*, Oxford, UK, pp. 779-788, 1996.

[7] A.R Bartha, "Dry friction induced backward whirl: theory and experiment," *Proceedings 5th IFToMM Conf. Rotor Dynamics*, Darmstadt, pp. 756-767, 1988.

[8] L. Hawkins, A. Filatov, S. Imani, and D. Prosser, "Test results and analytical predictions for rotor drop testing of an active magnetic bearing expander/generator," *ASME Journal of Engineering for Gas Turbines and Power*, Vol.129, pp. 522-529, 2007.

[9] H. Ulbrich, A. Chavez, and R. Dhima, "Minimization of contact forces in case of rotor rubbing using an actively controlled auxiliary bearing," *Proceedings 10th Int. Symp. Transport Phenomena and Dynamics of Rotating Machinery*, Honolulu, Hawaii, pp. 1-10, 2004.

[10] H. Ulbrich, and L. Ginzinger, "Stabilization of a rubbing rotor using a robust feedback control," Paper-ID: 306, *Proceedings 7th IFToMM Conf. Rotor Dynamics*, Vienna, Austria, 2006.

[11] I.S. Cade, M.N. Sahinkaya, C.R. Burrows, and P.S. Keogh, "On the design of an active auxiliary bearing for rotor/magnetic bearing systems," *Proceedings 11th Int. Symp. Magnetic Bearings*, Nara, Japan, 2008.